Analyst

RSC Publishing

PAPER

View Article Online
View Journal | View Issue

Cite this: *Analyst*, 2013, **138**, 1353

Impact of charge state on gas-phase behaviors of noncovalent protein complexes in collision induced dissociation and surface induced dissociation†

Mowei Zhou,‡ Shai Dagan§ and Vicki H. Wysocki‡*

Charge states of noncovalent protein complexes in the gas phase are known to affect their propensity for unfolding and dissociation. In this work, C-reactive protein (CRP) pentamer and Concanavalin A (ConA) tetramer at different charge states were subjected to collision induced dissociation (CID) and surface induced dissociation (SID) in a modified quadrupole/ion mobility/time-of-flight mass spectrometer. Charge manipulation was achieved through solution addition of charge reducing (triethylammonium acetate) or supercharging (3-nitrobenzylalcohol) reagents. The results show that charge reduction increases the stability of the proteins to dissociation and suppresses unfolding of the precursors. While CID becomes less effective at dissociation of charge reduced CRP and ConA, SID showed better preserved subunit contacts that are useful for quaternary structure elucidation. In contrast, supercharging of CRP and ConA leads to facile dissociation into subunits even for CID. The extent of precursor unfolding also increases with greater charge. Another interesting finding is that low-charge multimer products (dimers, trimers, *etc.*) seem to be collapsed after being released from the complexes. Further investigation is necessary to fully understand this behavior. The data presented here suggest that charge manipulation can be used to "tune" the dissociation behavior of noncovalent protein complexes in order to obtain the most useful information desired for structural analysis.

Received 20th October 2012
Accepted 21st December 2012

DOI: 10.1039/c2an36525a

www.rsc.org/analyst

Introduction

Structural characterization of protein complexes using mass spectrometry (MS) has become a growing field with the help of soft ionization techniques such as nanoelectrospray, where the protein complexes can be transferred from physiological solutions into the gas phase with minimal disruption.[1,2] The stoichiometry of protein complexes can be unambiguously determined by accurate molecular weight measurement of the complexes by mass spectrometry. Additionally, ion mobility (IM), a gas-phase separation technique, has been interfaced with mass spectrometry instrumentation, resulting in great potential for structural characterization of proteins.[3] In IM, ions are driven by an electric field in a pressurized cell and migrate differentially based on their size, shape and charge. The drift time required for the ion to traverse the cell is related to the collisional cross-section (CCS) of the ion. CCS measurements provide insights to three dimensional conformations of protein complexes that cannot be obtained by mass spectrometry alone. Recent studies[4–7] have shown the effectiveness of comparing experimental CCS data to the ones calculated for candidate structures generated by molecular modeling, to elucidate quaternary structures of protein assemblies.

Furthermore, non-covalent interactions maintaining the complexes can be disrupted in a controlled manner in the gas phase to release subunits for further structural analysis in tandem mass spectrometry (MS/MS) experiments. This disruption is commonly achieved by collisional activation of analytes with neutral inert gas targets such as argon or nitrogen and is known as collision induced dissociation (CID). It has been reported that a majority of protein complexes undergo unfolding upon CID, releasing highly charged, unfolded monomers from the original complexes.[8] Alternatively, the analytes can be activated by collision with a surface target (surface induced dissociation, SID). Previous studies from our group[8–10] have shown that SID provides unique protein quaternary structure information that is complementary to CID. It has also been shown recently that protein complexes which only differ in conformation and cannot be readily distinguished by mass or CID, dissociate differently in SID.[11] This behavior, featuring low charged, compact monomers as exhibited by the SID spectra of

Department of Chemistry and Biochemistry, University of Arizona, 1306 E. University Blvd., PO Box 210041, Tucson, Arizona, USA. E-mail: wysocki.11@chemistry.ohio-state.edu

† Electronic supplementary information (ESI) available: Fig. S1–S5 including scheme of instrument setup and supporting data. See DOI: 10.1039/c2an36525a

‡ Current address: Department of Chemistry and Biochemistry, Ohio State University, 484 W. 12th Ave., Columbus, Ohio, USA.

§ Permanent address: Israel Institute for Biological Research (IIBR), POB 19, Ness Ziona 74100, Israel.

several tetrameric and pentameric complexes, has been hypothesized[10] to be attributed to the fast, ~ single collision, high energy deposition from surface impact. We have recently incorporated an SID device into a commercial mass spectrometer with IM capability to monitor the conformation of subunit products released from protein complexes upon CID/SID.[12] The data show, for example, that a pentameric protein complex, C-reactive protein (CRP) dissociates into monomers with native-like CCS by SID with much less conformational rearrangement of the precursor than by CID. In general, it is beneficial to minimize conformational disruptions such as unfolding in the dissociation process so that native protein structures are better reflected.

Although CCSs from IM experiments on precursors of protein complexes sprayed under physiological conditions have been shown to be in good agreement with calculated CCSs of atomic structures (determined by X-ray crystallography or nuclear magnetic resonance) for a variety of protein complexes,[13] discrepancies are frequently observed for dominant highly charged monomer products released from the precursors upon CID.[12,14] High charge states of protein monomers are well-correlated with extended structures as shown by a number of IM and MS studies.[15–18] In contrast, the conformations of larger multimeric protein complexes may not extend significantly at elevated charge states.[7,19] Interestingly, compaction of a protein complex from native conformation was reported for an 11-membered ring protein (trp RNA-binding attenuation protein) at high charge states,[20] and we have also observed very similar behavior on another dodecameric protein complex (small heat-shock protein 16.9 from *Triticum aestivum*) in our laboratory.[21,22] This suggests that excess charge on the protein complexes might induce structural rearrangement, away from native conformation, in the gas-phase.

Consequently, solution additives that can reduce the charge states of protein complexes in electrospray have been used,[14,23] with the goal of better preserving the protein complexes in their native-like conformations. Pagel *et al.*[14] reported that a tetrameric protein complex transthyretin (TTR) exhibits suppressed unfolding and dissociation by CID at charge states lower than the normally observed +15 charge state. Lower charged compact monomers could be detected for lower charged precursors. Complete resistance to unfolding within accessible CID collision energies was observed when the charge state of TTR tetramer was below +11. Covalent peptide fragmentation from the protein backbone started to dominate CID spectra over subunit ejection when the charge was further reduced to +9. In another publication by Hall *et al.*,[7] a charge reduced pentameric complex, serum amyloid P (SAP), exhibited unusual compaction upon CID before unfolding. From their molecular dynamics simulations, the compaction was thought to originate from the collapse of the cavity of the native pentamer ring conformation. The data for precursors at a range of different charge states indicate that this conformational change is highly charge state dependent, and compaction at high charge states is unlikely due to Coulombic repulsion for SAP.[7] It was proposed that charge states of protein complexes affect potential barriers of unfolding and compaction processes. In addition, charge states affect the dissociation patterns observed in the mass spectra, as has also been shown in a previously reported example, where supercharging (*i.e.* increase the observed charge states of proteins in mass spectra by solution additives) is speculated to induce more dissociation into subunits with less unfolding in CID.[24]

In the present work, we present CID/SID and IM data of two protein complexes at "normal", reduced, and elevated charge states to further explore the effect of charge state on protein unfolding/dissociation in SID. CCSs of compact subcomplex products released in SID were compared with calculated values from crystal structure models, to investigate possible structural rearrangements of the ions in the gas-phase compared with their crystallographic conformations.

Experimental section

Reagents

Recombinant human C-reactive protein (CRP) from *E. coli* and serum amyloid P (SAP) from human serum were purchased from CalBiochem (EMD Biosciences, Inc., San Diego, CA). Concanavalin A (ConA) from *Canavalia ensiformis*, transthyretin (TTR) from human plasma, and glutamate dehydrogenase (GDH) from bovine liver were purchased from Sigma (Saint Louis, MO). The protein samples were buffer exchanged into 100 mM ammonium acetate using size exclusion spin columns (BioRad, Hercules, CA) without any further purification. The concentrations of the protein complexes were 8 μM for the CRP pentamer, and 50 μM for the ConA tetramer (in equilibrium with its dimer in solution). The molecular weights of the monomers are 23.0 kDa and 25.6 kDa for CRP and ConA, respectively. Ammonium acetate (EMD Chemicals Inc., Gibbstown, NJ) and 3-nitrobenzyl alcohol (>99%, Alfa Aesar, Ward Hill, MA) were dissolved in deionized water to a concentration of 100 mM. 100 mM triethylammonium acetate (TEAA) was prepared by mixing triethylamine (>99%, Sigma-Aldrich, Milwaukee, WI) and glacial acetic acid (>99.7%, EMD Chemicals Inc., Gibbstown, NJ) in deionized water with pH adjusted to 7. For charge manipulation experiments, 100 mM TEAA (for charge reduction[25,26]) or 100 mM 3-nitrobenzyl alcohol (3-NBA, for supercharging[27]) was added into the protein solution in 100 mM ammonium acetate (AA) at 20% by volume before MS analysis. For "normal" charged samples, 100 mM AA was added to 20% by volume to equalize the changes in protein concentrations.

Instrument modification and operation

The quadrupole-IM-time-of-flight (Q-IM-TOF) mass spectrometer (Waters Corporation, Manchester, UK) was modified as described elsewhere.[12] Briefly, the original trap traveling wave ion guide (TWIG) was replaced with a truncated TWIG. A custom SID device was inserted after the truncated TWIG and before the IM cell in the instrument chamber. Detailed design of the SID device was reported previously as part of another modification where the same SID device was placed after the IM cell.[11] Under normal operation, the trap and transfer TWIGs are

filled with argon (4 mL min^{-1}), and the IM cell is filled with nitrogen (60 mL min^{-1}) for separation of ions. The pressurized helium cell (120 mL min^{-1}) is used to kinetically cool and focus the ions before IM for higher resolution in mobility separation.[28] A detailed description of the instrument settings can be found in Fig. S1.† For MS and CID experiments, the voltages on the SID lenses are tuned to allow fly-through transmission of all the ions (Fig. S1b†). Packets of precursors in MS experiments, or packets of products in CID experiments are pulsed directly into the helium cell from the exit of the trap TWIG. For SID experiments, the voltage of the deflector is raised to steer the ions toward the surface target (Fig. S1a†). The other voltages on the SID lenses are tuned to collect the products and transfer them into the IM cell. Precursors are pulsed from the trap TWIG exit and strike the surface. The emerging products are then guided into the helium cell for separation.

The laboratory frame collision energy (E_{lab}) is defined as:

$$E_{lab} = V_{acceleration} \times z$$

$V_{acceleration}$ is the acceleration voltage in CID/SID, and z is the charge state of the precursor. It is used in the following discussion to approximately gauge the relative collision energy for the same protein complex and activation method but corrected for the difference in charge states. Typical acceleration voltages used are 10–200 V for CID and 20–150 V for SID within the limit of the power supply of the instrument. E_{lab} of CID and SID cannot be directly compared, mainly due to different collision target masses and lack of quantitative understanding of the energy transfer processes for large protein complexes during collisions. Similarities in percent precursor survival provide one means of comparison between SID and CID.

Proteins were ionized using a nanoelectrospray source. The original sprayer was replaced with a custom static sprayer. The static sprayer conducts a high voltage (1.0–1.5 kV) to a platinum wire that is inserted into a glass capillary filled with protein solutions. Other typical instrument conditions used are: cone voltage 50 V; backing pressure 5–6 mbar; TOF analyzer pressure 6×10^{-7} mbar. The source was left at room temperature without heating.

Determination of collisional cross-section

Experimental CCSs are determined following a published protocol[29,30] using TTR tetramer, ConA tetramer, SAP pentamer, and GDH hexamer as calibration standards. For the CCS profiles of undissociated precursors after CID/SID, the data were obtained using a 250 m s^{-1} traveling wave in the IM cell. For the CCS plots of products, CCSs were obtained at IM traveling wave velocities of 250, 275, and 300 m s^{-1}, which generate calibration curves with squared correlation coefficients larger than 0.99. The CCSs of each analyte under the three different wave velocities were averaged for better accuracy as suggested by Salbo *et al.*[31]

Theoretical CCSs were calculated from crystal structures in Protein Data Bank (PDB) using Mobcal,[32,33] which includes three algorithms: projection approximation (PA), exact hard-sphere scattering (EHS), and trajectory method (TJM). PA is believed to intrinsically underestimate CCSs of large protein assemblies. EHS does not account for the size dependent variation of the interaction potential,[34,35] and TJM is computationally too expensive for large systems. Discrepancies of calculation from experiment have been observed frequently due to insufficient modeling of the physical potentials[34] and the inelasticity of proteins.[36] A scaled PA,[7,13] based on empirical data, is used here to correlate experimental CCS with model structures, with a desire to use Projection Superposition Approximation[34] when the algorithm becomes available in the future.

$$CCS_{calc} = 1.14 \times CCS_{PA}\left(\frac{m_{exp}}{m_{pdb}}\right)^{\frac{2}{3}}$$

CCS_{calc} is the calculated CCS used for comparison to experimental data; CCS_{PA} is the calculated CCS from PA algorithm in Mobcal; m_{exp} is the experimental mass of the protein; m_{pdb} is the mass of the protein in the atomic structure. The atomic structures are obtained from PDB (PDB IDs are 1GNH for CRP, 3CNA for ConA). Missing hydrogen atoms were added to all the crystallography structures using autoPSF generator module in VMD.[37] No extra energy minimization of the atomic structures was performed. Theoretical CCSs of subcomplex structures (*e.g.* monomer, dimer, trimer) were obtained by calculating the subunit clusters clipped from the atomic structures of native assemblies. The collapsed trimers and tetramers of CRP were generated in PyMoL by rearranging the position of the subunits. Mobcal calculations were performed on the high performance computing systems at the University of Arizona. The current analysis is only intended to make qualitative conclusions on the trend of structural changes for large protein systems in the gas phase. More sophisticated simulations to generate the candidate structures will be performed in future work.

Results and discussion

Reduced charge state allows dissociation of CRP with minimal structural rearrangement of precursor and enhanced preservation of subunit contacts of products by SID

A dominant charge state of +24 for CRP was observed when spraying from AA. When TEAA was added, the dominant charge state was reduced to +18. These two precursors were examined with CID and SID. The conformational changes of the activated but undissociated protein precursors after activation by CID/SID at different charge states were first examined as shown in Fig. 1a–c. The colors of the spots represent normalized precursor survival yields in the spectra at each collision energy in order to visualize the extent of dissociation along with the change in CCS (warm/red colors for higher survival and cold/blue colors for lower survival of precursor).

The remaining precursor for +24 CRP can hardly be detected in SID even at very low acceleration voltages, thus only +18 is shown here for SID (Fig. 1a). It can be clearly seen that most of the +18 CRP dissociated without change in CCS below 0.5 keV, which has been presented previously in our recent report.[12] At higher E_{lab}, a slight decrease (at 0.7 keV) and subsequent increase (at 0.9 keV) in CCS can be observed where the precursor

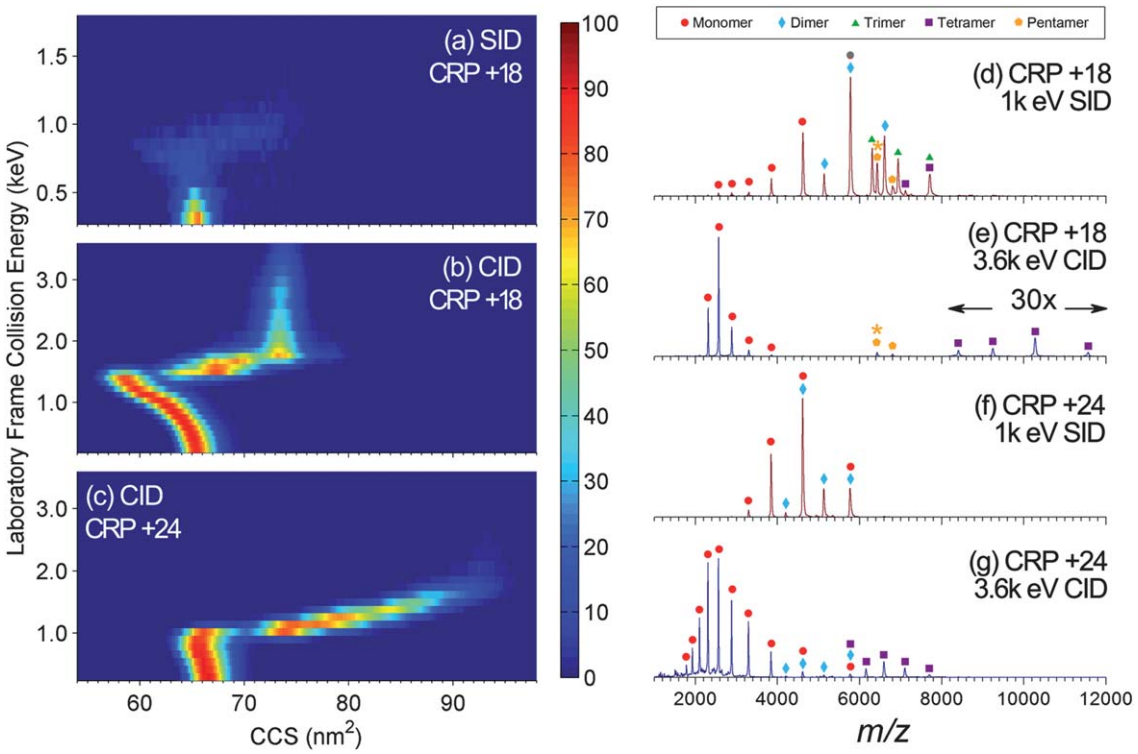

Fig. 1 CCS profiles of remaining +18/+24 CRP precursors upon (a) SID and (b and c) CID. SID of CRP +24 is not shown because the +24 precursor readily dissociates even at very low E_{lab}. The color scheme in the profiles (scale shown in the middle) shows the relative abundance of the precursor in the spectra. Both +18 and +24 CRP show distinct structural rearrangement upon CID. However, precursor depletion in SID is achieved at much lower E_{lab} with minimal conformational change. Representative (d and f) SID and (e and g) CID spectra for +18/+24 CRP. All major products are labeled using the scheme in the legend. Remaining precursors are labeled with asterisks to distinguish them from charge-stripped pentamers. A variety of products at different oligomeric states are detected in SID, with the +18 precursor featuring more large oligomers (*i.e.*, trimer, tetramer). CID exhibits the typical dissociation pattern of ejection of higher charged monomers than SID for precursors at both charge states.

constitutes less than 10% of the spectra, suggesting compaction and unfolding of the structure under these conditions. We suspect this could be at least partially attributed to collisions of the remaining precursors with some background gas, given the fact that a similar CCS change can be observed by acceleration at higher voltages in the SID region without striking the surface.

In contrast to the minimal CCS change in SID, undissociated precursors for both +18 and +24 CRP exhibit extensive transformations of CCS in CID (Fig. 1b and c). The precursors at the two different charge states do not seem to share identical unfolding pathways and unfold to different extents, with the higher charged precursor unfolding more extensively as indicated by larger CCSs. Compaction before unfolding is observed for both charge states, with much more pronounced compaction for the lower charged precursor. The compaction behavior has been already demonstrated to originate from the collapse into the center cavity of the ring structure for another pentameric protein complex[7] in the same pentraxin family as CRP. For precursors with more charge, the compaction pathway is likely to be suppressed due to a high energy barrier from Coulombic repulsion. An interesting feature is that the protein complex seems to start dissociating in CID only after it starts to unfold, as shown by the synchronized fading of color and increases in CCS in Fig. 1b and c.

Differences between dissociation for CRP at "normal" charge states of +24 (sprayed in AA) and reduced charge states of +18 (with TEAA added) are illustrated by representative MS/MS spectra shown in Fig. 1d–g. SID of +18 and +24 CRP both show dominant low charged (high m/z) monomer and dimer products (Fig. 1d and f). Considerable populations of trimers and tetramers are also observed from SID of the +18 precursor at the same E_{lab}. The appearance of trimers and tetramers in SID is thus an indication of better preservation of subunit interactions, further supported by the remaining precursor in the spectrum of +18 CRP which accounts for about 6% of the total signal. The additional products allow more subunit contacts to be revealed for topological studies, and this is especially useful in characterization of heterogeneous complexes.[9] The overall qualitative pattern of CID or SID spectra does not show strong dependence on collision energies within the range investigated (Fig. S2†). In CID, dissociation into subunits is insignificant at E_{lab} of 1 keV or lower for both charge states. Thus, the CID spectrum of +18 CRP at 3.6 keV, which gives the same precursor survival yield of 6% as shown for SID, is shown in Fig. 1e, featuring higher charged monomer products than those seen in SID. This pattern of highly charged monomers and complementary $(n - 1)$-mers has been observed in CID for many protein complexes, and is rationalized to involve an unfolded monomer leaving the complex.[8,9,16,38–40] At

the same E_{lab} of 3.6 keV, a similar dissociation pattern is maintained for CID of +24 CRP (Fig. 1g) as was seen for CID of +18 CRP, but with a broader charge state distribution of monomers and higher charged tetramers. A minor contribution from dimers is also observed. Overall, Fig. 1 illustrates that reduced charge state allows dissociation of CRP with minimal structural rearrangement of precursor and enhanced preservation of subunit contacts of products by SID, while monomer and tetramer are the dominant products of CID.

Quaternary structure studies of ConA by SID are not limited by the reduced charge state although dissociation is greatly suppressed in CID

Similar CID/SID experiments were carried out for ConA. The dominant charge state of ConA was +19 in AA, and shifted to +13 with the addition of TEAA. The CCS profiles of the undissociated precursors and corresponding spectra for +13/+19 ConA upon CID/SID are illustrated in Fig. 2. The +13 precursor starts to dissociate at low E_{lab} in SID with minimal change in CCS (Fig. 2a). At higher E_{lab} (0.5 keV and above), populations of precursors that undergo compaction and those that undergo unfolding are observed simultaneously. The compaction and unfolding proceed until the precursors are fully depleted. In comparison, CID of +13 ConA shows mainly compaction and resistance to unfolding/dissociation even at high E_{lab} (Fig. 2b). Although ConA tetramer is known to have a carbohydrate binding cavity from its crystal structure,[41] it is not clear if the compaction of ConA follows the same explanation of collapsed internal cavity for SAP[7] because it has a very different fold from SAP and CRP. It is noted that although collision with background gas might contribute to the small percentage of compaction observed in SID of +13 ConA, the increase in CCS at high SID energies cannot be attributed to gas collisions because no unfolding was observed in CID. The drastic difference of the CCS profiles between CID and SID suggests that SID is able to access pathways (*e.g.* unfolding and dissociation of +13 ConA) that are not available for CID at the same magnitude or within the maximum accessible range of E_{lab} in the instrument.

The lower dissociation propensity of the ConA tetrameric complex enables the precursor CCS to be monitored also at higher charge in SID. The +19 ConA produces more than one unfolding intermediate in both CID and SID (Fig. 2c and d), but complete dissociation was achieved in SID prior to formation of further unfolded intermediates observed in CID (74 nm^2 and 83 nm^2). These data with CRP and ConA all show the same trend of increased resistance to dissociation and unfolding at reduced charge states, which is consistent with previous findings in the literature.[14] More importantly, for both proteins the precursor CCSs after collisions are better maintained in SID with charge

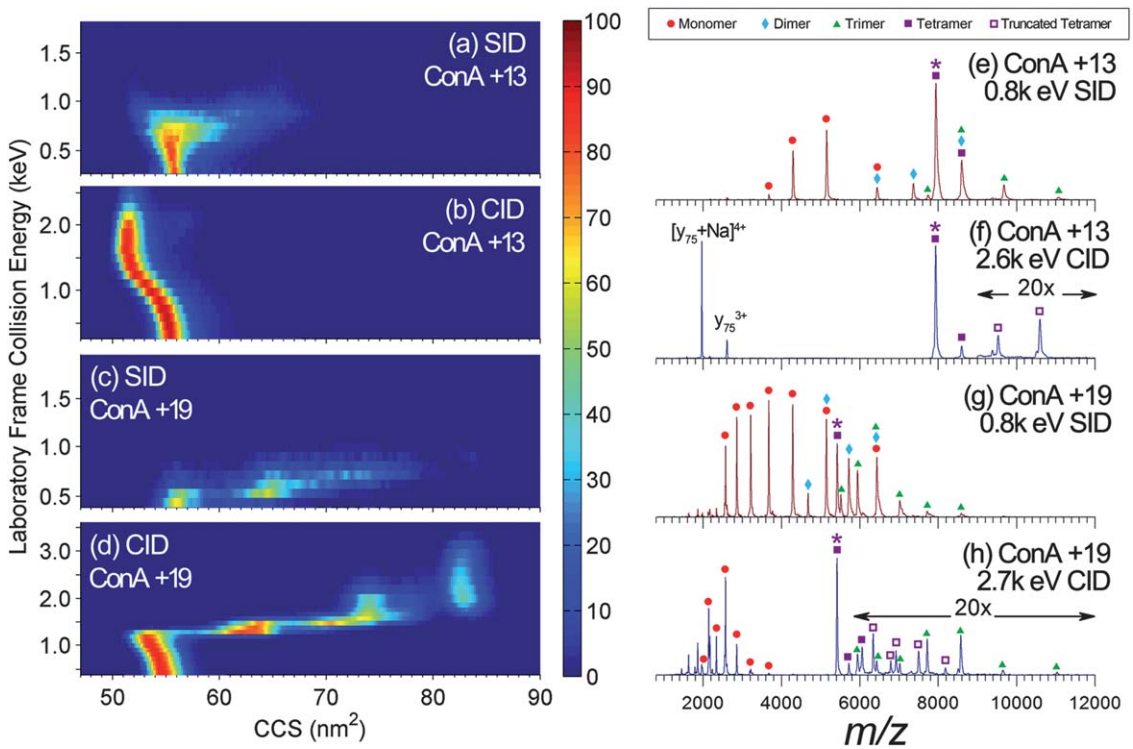

Fig. 2 CCS profiles of remaining +13/+19 ConA upon (a and c) SID and (b and d) CID. The color scheme in the profiles (scale shown in the middle) shows the relative abundance of the precursor in the spectra. Each of the profiles shows a distinctly different behavior of structural rearrangement upon activation. Again, precursor depletion in SID is achieved at much lower E_{lab} than the CID counterparts before extensive conformational changes occur. Representative (e and g) SID and (f and h) CID spectra for +13/+19 ConA. All major products are labeled using the scheme in the legend. Remaining precursors are labeled with asterisks, and open purple squares are truncated tetramers due to peptide ejection. SID shows extensive dissociation into subunits, while significant peptide loss from the protein complex is observed in CID. At the charge state of +13, production of the peptide fragments is the major pathway in the CID spectrum.

reduction. The remaining precursor of CRP +18 after SID did not show any significant change in CCS even when most of it had dissociated. Although unfolding is not eliminated for SID of +13 ConA, the change in CCS of the remaining precursor is accompanied by substantial decrease of precursor signal (*i.e.* precursor dissociation). This is in contrast with the CID behavior of +13 ConA where no dissociation into subunits is observed when CCS of the precursor begins to decrease above 1 keV. While unfolding is suppressed for lower charged precursors also for CID, the compaction pathway prior to dissociation generates conformations that may still not reflect the original quaternary structures.

SID spectra of the +13 and +19 ConA precursors (Fig. 2e and g) both demonstrate extensive dissociation to monomers, dimers, and trimers at E_{lab} of 0.8 keV. Again, the overall pattern of CID or SID spectra, respectively, does not vary substantially within a range of collision energies studied (Fig. S3†), and at E_{lab} of 0.8 keV no dissociation can be observed in CID. For the CID spectrum of +13 ConA at 2.6 keV, which gives the same abundance of around 40% remaining precursor as 0.8 keV SID, only a peptide loss of 7.8 kDa (y_{75}) can be observed (Fig. 2f). It is noted that both the +3 and +4 y_{75} present as multiple peaks corresponding to different additions of small salt cations, which is common in native mass spectrometry. Only the identities of the most abundant peaks are labeled. For the "normal" charged +19 ConA, in addition to the typical CID pattern of highly charge monomers and complementary trimers, the CID spectrum shows peptide fragments in the low *m*/*z* region and tetramers missing parts of the intact mass (loss of 7.8 kDa or 12.9 kDa, only the truncated tetramers are labeled for simplicity) in the high *m*/*z* region (Fig. 2h). ConA is known to have naturally unligated monomers consisting of two non-covalently associated large peptide fragments during post-translational modification,[42,43] and the C-terminal piece is labile in acid.[44] The occurrence of incomplete ligation in the ConA sample was verified by the MS spectrum of denatured ConA, which showed both the intact monomer (25.6 kDa) and the unligated peptide pieces (12.9 kDa for the N-terminal piece, 12.7 kDa for the C-terminal piece, spectrum not shown). Therefore, we propose that the 7.8 kDa peptide (y_{75}) possibly comes from covalent fragmentation of the labile site on the C-terminal piece, assisted by protonation. The ejection of the 12.9 kDa peptide correlates well with the mass of the naturally unligated N-terminal peptide piece. This unique behavior of peptide ejection in CID can be rationalized by unfolding of the tertiary structure and subsequent release of the non-covalently bound peptide fragment.

For the lower charged ConA (+13, Fig. 2f) which did not experience significant unfolding (Fig. 2b), cleavage of the labile peptide was observed instead. The fact that peptide ejection is hardly detectable in SID implies that perturbation of the non-covalently assembled monomer is minimized during dissociation. Overall, charge reduction increases the stability of protein complexes but also limits the quaternary information obtainable from dissociation by CID. SID of charge reduced precursors, on the other hand, provides extensive dissociation with better preserved noncovalent contacts that are useful for quaternary structure studies without spectral complications of peptide fragments.

High-order oligomeric products undergo compaction in the gas phase

CCSs of subunit products from differently charged precursors as a function of charge state of each product were examined. We found that CCSs of products are correlated well with their charge state, and CCSs for a given charge state are largely independent of collision energy or activation method under the current experimental conditions. However, decrease in CCS as a function of increasing collision energy just above the dissociation onset energy has been observed for a few large oligomeric products of CRP (data not shown), which is likely due to compaction of low charged ions and deserves further investigation in future experiments.

The data shown in Fig. 3 are CCSs for the dominant products observed in the mass spectra of CRP and ConA discussed earlier (in Fig. 1 and 2). The correlation between CCS and charge state has been reported in our previous work for some monomer products,[12] and are illustrated in the trends shown in Fig. 3. As expected, the charge state distributions of major products change with precursor charge states and activation methods. Because CID produces a broader range of charge states and higher charge states than SID, CCSs of subunit products from CID of CRP and ConA decrease with a decrease in charge state and reach a plateau below a certain "transition" charge state (Fig. 3a and c). Most products in SID reside in the plateau region where the ions are also lower charged (Fig. 3b and d). The same CCSs can be observed for products at the same charge states, regardless of the charge states of the precursors. Rather, charge states of all products shift downwards when the charges of the precursors are reduced (*i.e.*, open symbols *vs.* filled symbols).

When compared to calculated CCSs of subunits clipped from crystal structures, all monomer products in SID and corresponding lower charged ones in CID show good agreement between experimental CCSs and the calculations. This implies that these low charged monomers, predominantly generated by SID, have retained nativelike conformations after departing the complexes. However, CCSs of the compact dimers for both CRP and ConA in the plateau region are all slightly lower than the calculated values. This discrepancy of CCS is unlikely to be attributed to errors in experiment or calculation, because the ConA dimers in equilibrium with ConA tetramers sprayed directly from solution have larger CCSs that are consistent with the calculations (Fig. S4†). Thus, it is possible that the dimers have collapsed during or after dissociation of the precursor. This is further supported by the fact that the solution ConA dimers at relatively lower charge states collapse upon activation (data not shown). Similarly, ConA trimer products (43 nm^2) exhibit slight compaction compared with the clipped trimer structure (46 nm^2).

Interestingly, CCSs of the trimers (40 nm^2) in SID for +18 CRP deviate from the calculated clipped trimer (46 nm^2) more significantly than the compaction seen for ConA trimers, in spite of the similar size of the two types of trimers. Likewise, deviation in CCS can be seen for CRP tetramer products (48 nm^2 for the SID product *vs.* 58 nm^2 for the clipped tetramer). The experimental CCSs are in better agreement with the calculation if the trimer and tetramer have undergone structural rearrangement into

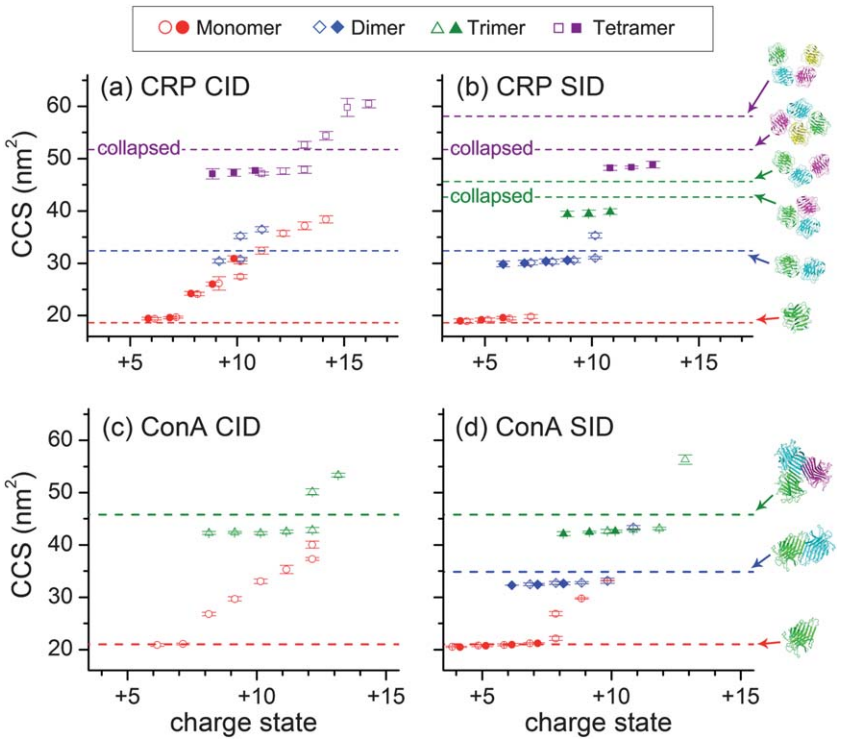

Fig. 3 CCS plots of CRP products from (a) CID and (b) SID, as well as CCS plots of ConA products from (c) CID and (d) SID as a function of charge state of the products. Open symbols are products from normal charged precursors (+24 CRP and +19 ConA); filled symbols are products from reduced charged precursors (+18 CRP and +13 ConA). Dashed lines are calculated CCSs from corresponding model structures shown as insets. Most SID products are compact and low-charged. Products larger than monomers show some collapse from the clipped structures. Additionally, CRP trimer and tetramer products seem to rearrange themselves as indicated by the substantial decrease in CCS from the clipped structures. In contrast, a majority of CID products show expansion in CCS with increasing charge, indicative of gradual unfolding.

more compact conformations with less exposed surface area (43 nm^2 and 52 nm^2, respectively). This is reasonable because the clipped CRP trimer and tetramer are unlikely to be the most stable conformations at the time scale of IM analysis (milliseconds). The loss of binding partners might induce relocation of subunits to "bury" the exposed binding region for the lowest energy possible. The less pronounced compaction for ConA is possibly due to a more rigid quaternary structure which is stable even when one or a few subunits are removed. Alternatively, the ConA trimer may have rearranged into a different conformation from the clipped trimer but the CCS did not change significantly enough to be manifested by the measurement.

It is noted that the more extended structure of the CRP tetramer product +13 in CID with a CCS of 53 nm^2 (the upper of the two purple diamonds at the charge state of +13 in Fig. 3a) does not necessarily relate to the collapsed tetramer model even though their CCSs show a reasonable match. The more extended +13 CRP tetramer product in CID can be alternatively attributed to a partially unfolded collapsed tetramer, which keeps unfolding at charge states higher than +13 just like the trend for the unfolding monomers with increasing numbers of charge. It would be interesting to further study the conformational stabilities of these oligomeric products, which can only be isolated in the gas phase, with molecular dynamics simulations and more accurate CCS algorithms to better elucidate their structures.

Supercharging enhances unfolding of precursors and dissociation of oligomeric products

In addition to the "normal" charging and reduced charging conditions, we also examined unfolding and dissociation behaviors in SID/CID when the precursor is supercharged with the addition of 3-NBA to the spraying solution to form CRP +28 and ConA +23. In contrast to some monomeric proteins which supercharge from unfolding,[15] CCSs of CRP and ConA precursors do not change remarkably within the charge states examined (Fig. S4†). Preservation of nativelike CCS was already reported for supercharged SAP pentamer, but did not apply to alcohol dehydrogenase tetramer.[45] Supercharged CRP and ConA expand to larger CCSs than the lower charge states (shown earlier in Fig. 1 and 2) without noticeable compaction in CID (Fig. S5†). Dissociation into subunits also becomes more extensive, thus monitoring remaining precursor in SID is difficult due to precursor depletion, together with unfolding caused by background gas collisions even at low E_{lab}. Representative CID/SID spectra are shown in Fig. 4 at E_{lab} similar to those in Fig. 1 and 2. For CRP +28, the SID spectrum (Fig. 4a) did not change significantly from the CRP +24 (Fig. 1f), except that the abundance for dimers is decreased and the dominant monomer product is shifted by one charge state higher. On the other hand, the CID spectrum of CRP +28 features a wide charge state distribution of monomer products and an increased abundance

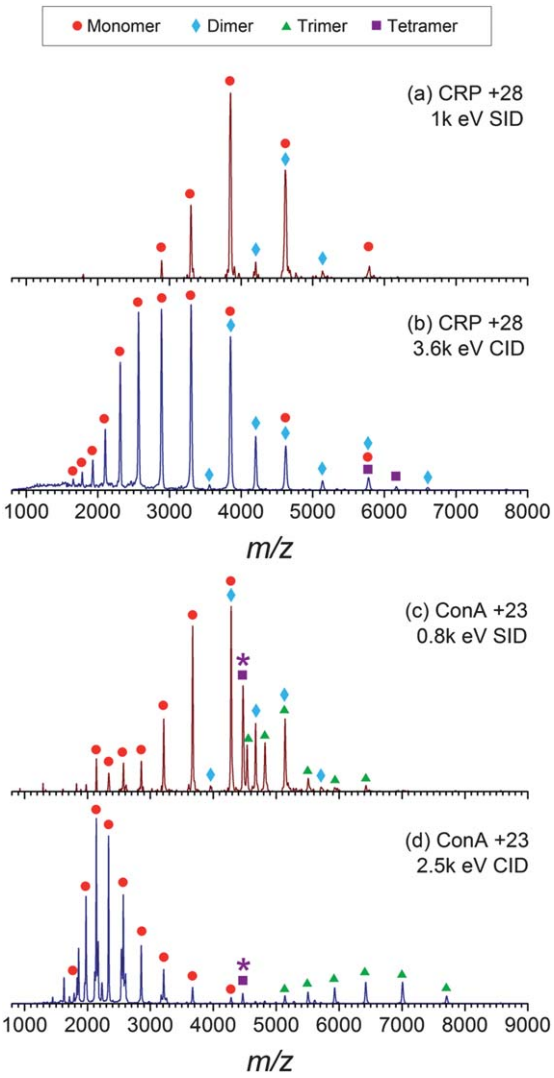

Fig. 4 SID/CID spectra of (a and b) supercharged CRP and (c and d) supercharged ConA at E_{lab} comparable to the previous SID and CID spectra at lower charge states (Fig. 1d–g and 2e–h). With supercharging, CID shows more extensive dissociation than the precursors at lower charge, with suppressed levels of peptide ejection.

of dimer products that are different from CRP +24 and +18. Similar results have been reported for SAP where dimer products, atypical for CID of "normal" charged precursors, were detected for the supercharged precursor.[7]

More interesting results can be observed for supercharged ConA, especially in CID where peptide ejection is greatly suppressed (Fig. 4d). Monomer ejection, typical for CID of other protein complexes, is the prevalent pathway observed for supercharged ConA. SID of supercharged ConA (Fig. 4c) shows products (monomer, dimer, trimer) similar to the SID of "normal" charged ConA (Fig. 2g). The major difference is the significantly lower abundance of highly charged, unfolded monomer products in the low m/z region of the SID spectrum for the supercharged precursor. Dissociation is favored at this charge state over unfolding that can lead to the ejection of peptide fragments of unligated monomers in CID, presumably due to a lower energy barrier of dissociation relative to unfolding of supercharged ConA. This is reminiscent of the finding by Yin and Loo[46] that top-down experiments of supercharged protein–ligand complexes yield more fragments retaining ligands.

It can be concluded that supercharging facilitates dissociation of protein complexes, based on the following experimental observations: (1) fewer dimers preserved in SID of supercharged CRP which is presumably caused by enhanced secondary dissociation, with the dimers further dissociating into monomers; (2) enhanced dissociation into multimers in CID manifested by the appearance of dimers for supercharged CRP. The ease of dissociation is accompanied by decreased quaternary conformational stability of the complexes as indicated by the augmented expansion of precursor CCSs upon activation. The increases in CCSs appear to contradict the observation of better preserved tertiary folds, as manifested by the smaller population of unfolded monomer products for supercharged CRP by SID and diminished peptide ejection for supercharged ConA by CID. However, the larger increase in CCS for supercharged precursor may be rationalized by an alternative unfolding pathway of conformational expansion other than exclusive unfolding of a monomer. We also observe a small population of compact trimers for CID of supercharged CRP at high E_{lab}, with CCS similar to those released in SID of charge reduced precursor (data not shown), which is likely to result from secondary dissociation of tetramer products. Further investigation with a greater number of protein systems is necessary to understand the change of dissociation behavior of supercharged protein complexes.

Rationalizing the influence of charge state on gas-phase protein complexes

The data presented here suggest that different unfolding and dissociation pathways of noncovalent protein complexes can be accessed by charge manipulation. Charge reduction has been shown to increase the stability of nativelike conformations of protein complexes in the gas phase,[7,14] consistent with the reduced unfolding and dissociation observed for CRP and ConA at reduced charge states in this work. The increased stability of these complexes leads to insufficient dissociation in CID for quaternary structure elucidation. Additionally, compaction of the complexes upon activation became the dominant pathway in CID, possibly due to the lower energy barrier from less Coulombic repulsion at reduced charge, as supported by molecular dynamics simulations by Hall *et al.*[7] In contrast, extensive dissociation into subunit products can be still observed in SID for charge reduced precursors, but with less unfolding and better preserved multimers. This is beneficial in the sense that dissociation into subunits, particularly into multimer products, can be achieved in SID with minimal conformational rearrangement, so that the dissociation data would better reflect protein structures in the native states.

CCS measurements of products from CRP and ConA (normal charge and reduced charge) indicate that multimers released from the complexes undergo compaction from their spatial arrangements in the native states during or after dissociation.

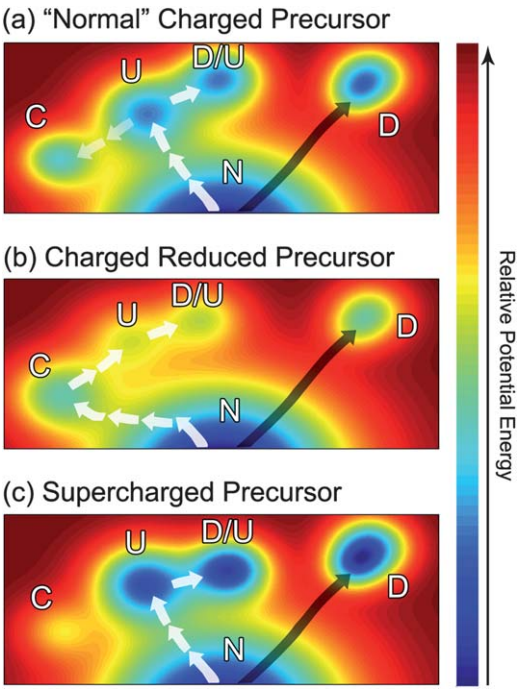

Fig. 5 Hypothetical potential energy diagram of a protein complex for (a) normal charged, (b) charge reduced, and (c) supercharged precursors. The color scale shown on the right is arbitrary for this qualitative presentation, where blue represents the lower energy states. White arrows indicate major pathways in typical low-energy CID experiments with stepwise energy deposition. Black arrows represent the major SID pathway with high energy deposition that overcomes high energy barriers. The potential wells are labeled as follows: N – nativelike state; C – compaction/collapsed state; U – unfolded state; D/U – dissociation of unfolded subunits; D – direct dissociation with minimal unfolding. Charge reduction makes the protein more resistant to disruption as indicated by the elevated potential energies of all the disrupted states. Supercharging decreases the stability of the protein and lowers the energy barriers to unfolding and dissociation processes, but compaction pathways are suppressed.

Moreover, CRP trimer and tetramer products experienced even larger extents of collapse as indicated by the significant compactions compared with the clipped structures, with preliminary modeling indicative of subunit rearrangements. This compaction behavior of the subunit products raises the concern of structural relaxation of the subunits after dissociation. It is possible that proteins refold into more stable gas-phase, non-native conformations according to some experimental and theoretical studies.[45,47] A recent IM study has shown that upon charge reduction to only a few charges (+1 to +3), even the solution-denatured proteins adopt compact structures when transferred into the gas phase in the absence of Coulombic stretching.[48] Although low charge state is usually an indicator of compact conformations of protein complexes in the gas phase, the detailed correlation between "compact" and "native" conformations still deserves further investigation.

Another interesting observation is the change in dissociation behavior for the supercharged precursors. Some compact dimers and monomers can be detected in CID for supercharged CRP. Supercharged ConA shows enhanced monomer ejection at a greatly suppressed level of the peptide fragmentation that dominates the CID spectrum of charge reduced ConA. The enhanced precursor unfolding and dissociation from supercharging contrast with the increased stability of protein complexes at reduced charge states.

The effect of charge state on the behaviors of protein complexes in CID/SID is evident. It has been proposed, based on molecular dynamics simulations, that the relative energy barriers of unfolding, compaction and dissociation change with the number of charges.[7] A hypothetical plot of the energy diagram (Fig. 5) generalizes our current understanding of the impact of charge state on protein complexes based on the data discussed here and literature reports. Overall, an increased number of charges lowers the energy barriers of unfolding and dissociation, but increases the barrier for compaction. Upon a certain amount of internal energy deposited, protein complexes will either unfold, collapse, or dissociate based on which pathways are accessible for a given charge state. As opposed to supercharging where proteins are more readily dissociated but also more prone to unfolding, proteins become more resistant to dissociation at lower charge. However, the reduction in charge also makes compaction more prevalent.

Conclusions

In summary, it is beneficial to "tune" the energy landscapes of the protein complexes by charge manipulation in order to access the most informative dissociation pathways. Consistent with our previous hypothesis, the fast, energetic activation in SID makes a variety of pathways accessible. In contrast, prevalent pathways in CID are usually the ones with the lower energy barriers due to the stepwise, longer time scale and less efficient energy transfer under normal CID operating conditions. Because of the suppressed unfolding and better preserved subunit contacts, SID of charge reduced precursors is able to provide more information on protein quaternary structures.

Acknowledgements

We are grateful for financial support from the National Science Foundation (Grant 0923551 to VHW). An allocation of computer time from the UA Research Computing High Performance Computing (HPC) and High Throughput Computing (HTC) at the University of Arizona is gratefully acknowledged.

References

1 T. L. Pukala, *Aust. J. Chem.*, 2011, **64**, 681–691.
2 G. R. Hilton and J. L. P. Benesch, *J. R. Soc., Interface*, 2012, **9**, 801–816.
3 Y. Zhong, S.-J. Hyung and B. T. Ruotolo, *Expert Rev. Proteomics*, 2012, **9**, 47–58.
4 A. J. Baldwin, H. Lioe, G. R. Hilton, L. A. Baker, J. L. Rubinstein, L. E. Kay and J. L. P. Benesch, *Structure*, 2011, **19**, 1855–1863.
5 C. Uetrecht, I. M. Barbu, G. K. Shoemaker, E. v. Duijn and A. J. R. Heck, *Nat. Chem.*, 2011, **3**, 126–132.
6 A. Politis, A. Y. Park, S.-J. Hyung, D. Barsky, B. T. Ruotolo and C. V. Robinson, *PLoS One*, 2010, **5**, e12080.

7 Z. Hall, A. Politis, M. F. Bush, L. J. Smith and C. V. Robinson, *J. Am. Chem. Soc.*, 2012, **134**, 3429–3438.
8 R. L. Beardsley, C. M. Jones, A. S. Galhena and V. H. Wysocki, *Anal. Chem.*, 2009, **81**, 1347–1356.
9 A. E. Blackwell, E. D. Dodds, V. Bandarian and V. H. Wysocki, *Anal. Chem.*, 2011, **83**, 2862–2865.
10 C. M. Jones, R. L. Beardsley, A. S. Galhena, S. Dagan, G. Cheng and V. H. Wysocki, *J. Am. Chem. Soc.*, 2006, **128**, 15044–15045.
11 M. Zhou, C. Huang and V. H. Wysocki, *Anal. Chem.*, 2012, **84**, 6016–6023.
12 M. Zhou, S. Dagan and V. H. Wysocki, *Angew. Chem., Int. Ed.*, 2012, **51**, 4336–4339.
13 J. L. P. Benesch and B. T. Ruotolo, *Curr. Opin. Struct. Biol.*, 2011, **21**, 641–649.
14 K. Pagel, S.-J. Hyung, B. T. Ruotolo and C. V. Robinson, *Anal. Chem.*, 2010, **82**, 5363–5372.
15 H. J. Sterling, C. A. Cassou, A. C. Susa and E. R. Williams, *Anal. Chem.*, 2012, **84**, 3795–3801.
16 J. C. Jurchen and E. R. Williams, *J. Am. Chem. Soc.*, 2003, **125**, 2817–2826.
17 H. J. Sterling, C. A. Cassou, M. J. Trnka, A. L. Burlingame, B. A. Krantz and E. R. Williams, *Phys. Chem. Chem. Phys.*, 2011, **13**, 18288–18296.
18 D. E. Clemmer, R. R. Hudgins and M. F. Jarrold, *J. Am. Chem. Soc.*, 1995, **117**, 10141–10142.
19 C. J. Hogan Jr, R. R. Ogorzalek Loo, J. A. Loo and J. F. d. l. Mora, *Phys. Chem. Chem. Phys.*, 2010, **12**, 13476–13483.
20 B. T. Ruotolo, K. Giles, I. Campuzano, A. M. Sandercock, R. H. Bateman and C. V. Robinson, *Science*, 2005, **310**, 1658–1661.
21 A. E. Blackwell, M. Zhou and V. H. Wysocki, *59th Conference on Mass Spectrometry and Allied Topics*, Denver, CO, 2011.
22 A. E. Blackwell, Ph.D. thesis, University of Arizona, 2012.
23 R. Bornschein, S.-J. Hyung and B. Ruotolo, *J. Am. Soc. Mass Spectrom.*, 2011, **22**, 1690–1698.
24 E. B. Erba, B. T. Ruotolo, D. Barsky and C. V. Robinson, *Anal. Chem.*, 2010, **82**, 9702–9710.
25 D. Lemaire, G. Marie, L. Serani and O. Laprévote, *Anal. Chem.*, 2001, **73**, 1699–1706.
26 U. H. Verkerk, M. Peschke and P. Kebarle, *J. Mass Spectrom.*, 2003, **38**, 618–631.
27 S. H. Lomeli, S. Yin, R. R. Ogorzalek Loo and J. A. Loo, *J. Am. Soc. Mass Spectrom.*, 2009, **20**, 593–596.
28 K. Giles, J. P. Williams and I. Campuzano, *Rapid Commun. Mass Spectrom.*, 2011, **25**, 1559–1566.
29 M. F. Bush, Z. Hall, K. Giles, J. Hoyes, C. V. Robinson and B. T. Ruotolo, *Anal. Chem.*, 2010, **82**, 9557–9565.
30 B. T. Ruotolo, J. L. P. Benesch, A. M. Sandercock, S.-J. Hyung and C. V. Robinson, *Nat. Protoc.*, 2008, **3**, 1139–1152.
31 R. Salbo, M. F. Bush, H. Naver, I. Campuzano, C. V. Robinson, I. Pettersson, T. J. D. Jørgensen and K. F. Haselmann, *Rapid Commun. Mass Spectrom.*, 2012, **26**, 1181–1193.
32 M. F. Mesleh, J. M. Hunter, A. A. Shvartsburg, G. C. Schatz and M. F. Jarrold, *J. Phys. Chem.*, 1996, **100**, 16082–16086.
33 A. A. Shvartsburg and M. F. Jarrold, *Chem. Phys. Lett.*, 1996, **261**, 86–91.
34 C. Bleiholder, T. Wyttenbach and M. T. Bowers, *Int. J. Mass Spectrom.*, 2011, **308**, 1–10.
35 E. Jurneczko and P. E. Barran, *Analyst*, 2011, **136**, 20–28.
36 C. J. Hogan, B. T. Ruotolo, C. V. Robinson and J. Fernandez de la Mora, *J. Phys. Chem. B*, 2011, **115**, 3614–3621.
37 W. Humphrey, A. Dalke and K. Schulten, *J. Mol. Graphics*, 1996, **14**, 33–38.
38 E. D. Dodds, A. E. Blackwell, C. M. Jones, K. L. Holso, D. J. O'Brien, M. H. J. Cordes and V. H. Wysocki, *Anal. Chem.*, 2011, **83**, 3881–3889.
39 J. L. P. Benesch, J. A. Aquilina, B. T. Ruotolo, F. Sobott and C. V. Robinson, *Chem. Biol.*, 2006, **13**, 597–605.
40 F. Sobott and C. V. Robinson, *Int. J. Mass Spectrom.*, 2004, **236**, 25–32.
41 K. D. Hardman and C. F. Ainsworth, *Biochemistry*, 1972, **11**, 4910–4919.
42 J. L. Wang, B. A. Cunningham and G. M. Edelman, *Proc. Natl. Acad. Sci. U. S. A.*, 1971, **68**, 1130–1134.
43 D. M. Carrington, A. Auffret and D. E. Hanke, *Nature*, 1985, **313**, 64–67.
44 A. B. Edmundson, K. R. Ely, D. A. Sly, F. A. Westholm, D. A. Powers and I. E. Leiner, *Biochemistry*, 1971, **10**, 3554–3559.
45 Z. Hall and C. Robinson, *J. Am. Soc. Mass Spectrom.*, 2012, **23**, 1161–1168.
46 S. Yin and J. A. Loo, *Int. J. Mass Spectrom.*, 2011, **300**, 118–122.
47 K. Breuker and F. W. McLafferty, *Proc. Natl. Acad. Sci. U. S. A.*, 2008, **105**, 18145–18152.
48 A. Maisser, V. Premnath, A. Ghosh, T. A. Nguyen, M. Attoui and C. J. Hogan, *Phys. Chem. Chem. Phys.*, 2011, **13**, 21630–21641.

